Reactions between Li Atoms and RCN (R = H or CH_3): Semiempirical SCF MO and Matrix Isolation ESR Studies

Paul H. Kasai

Contribution from the IBM Research Division, Almaden Research Center, 650 Harry Road, San Jose, California 95120-6099

Received March 9, 1998

Abstract: Reaction passage between the Li atom and the HCN molecule and that between the Li atom and the CH_3CN molecule were examined by a semiempirical molecular orbital method (MNDO). For both systems two distinct passages were revealed; one leads to the formation of an end-on complex (**I**), HCN···Li, and the other to the formation of a side-on complex (**II**), $Li^+(HCN)^-$. The end-on complex is a weak, van der Waals type, while the side-on complex is a strong, charge-transferred type as indicated. An ESR study of argon matrices in which Li atoms and HCN (or CH_3CN) had been co-condensed revealed the presence of the two complexes in accord with the theoretical prediction. Irradiation of the matrix with near-IR light ($\lambda = 850 \pm 50$ nm) resulted in conversion of complex **I** to complex **II**. The *g* tensors and the hyperfine coupling tensors of the linear and side-on complexes observed in both the Li/HCN and Li/CH_3CN systems were determined. In complex **I** the unpaired electron is in an sp hybridized orbital of Li projected away from the ligand. In complex **II**, the unpaired electron is essentially in the in-plane antibonding π orbital of the C−N moiety.

Introduction

Recently we conducted a matrix isolation ESR study of the Al/HCl/argon system. The study revealed spontaneous formation of the insertion product, H−Al−Cl, as well as hydrogen atoms when Al atoms and HCl molecules were co-condensed in argon matrices at ∼4 K.[1] We also examined the possible reaction process(es) between the Al atom and the HCl molecule by a semiempirical SCF molecular orbital method, MNDO. The theoretical examination revealed that the Al atom and the HCl molecule would indeed react spontaneously at their electronic ground states. It further revealed that the insertion process, Al + H−Cl → H−Al−Cl, occurs when the Al atom approaches the hydrogen side of the HCl molecule, and that the displacement process, Al + Cl−H → Al−Cl + H, occurs when the Al atom approaches from the chlorine side.[1]

We also conducted earlier a matrix isolation ESR study of the Li/acetylene/Ar system, and observed the formation of the charge transferred, side-on complex depicted below.[2]

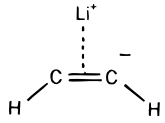

Here the unpaired electron resides in the in-plane antibonding π orbital of the (bent) acetylene moiety. It was therefore postulated that the complex was formed when the Li atom in its excited P state reacts with the acetylene molecule. A later (re)examination of the reaction by the semiempirical SCF molecular orbital method (MNDO) revealed, however, that the reaction could proceed with the Li atom in its S ground state. The theoretical study showed that the Li atom initially adds to the acetylene molecule to form an adduct of the vinyl form (as is known for the reaction between the hydrogen atom and the acetylene molecule). The charge transfer occurs as the vinyl form is achieved; the resulting Li ion then moves to the position of the side-on complex.[3]

The fact that the final products given by the semiempirical SCF molecular orbital method are in exact agreement with those determined experimentally for the two totally different systems adds some credence to the reaction passages predicted by the theory. In the case of the Al/HCl system, a recent ab initio study based on the density functional theory predicted the reaction passages in good agreement with those given by the semiempirical method.[4] We thence became enticed to look for a viable reaction system for which the experimental study had not been performed; if found, we would examine the system first by the theory followed by the experiment. We noted that the reaction between the Li atom and the HCN molecule had not been examined experimentally. The present paper reports on the result of examination of the reaction between the Li atom and the HCN molecule and also that between the Li atom and CH_3CN molecule first by the semiempirical SCF MO method and then by the matrix isolation ESR method. The theory predicted the formation of two distinct complexes, an end-on complex **I**, and a side-on complex **II**.

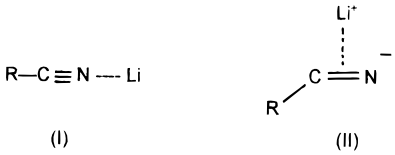

The end-on complex is a weak, van der Waals type, while the side-on complex is a strong, charge-transferred type as indicated.

(1) Köppe, R.; Kasai, P. H. *J. Am. Chem. Soc.* **1996**, *118*, 135.
(2) Kasai, P. H. *J. Am. Chem. Soc.* **1992**, *114*, 3299.
(3) Kasai, P. H. Unpublished result; shown curtly in the author's web page: www.almaden.ibm.com/st/people/kasai.
(4) Fängström, T.; Lunell, S.; Kasai, P. H.; Eriksson, L. A. *J. Phys. Chem.* **1998**, *102*, 1005.

S0002-7863(98)00790-2 CCC: $15.00
Published on Web 07/23/1998

The matrix isolation ESR study of the Li/HCN (or CH_3CN)/Ar system clearly revealed the presence of the two complexes in accord with the theoretical prediction. Irradiation of the matrix with near-IR light ($\lambda = 850 \pm 50$ nm) resulted in conversion of complex **I** to complex **II**.

Experimental and Computational Technique

A liquid helium cryostat that would allow trapping of vaporized metal atoms in an argon matrix and examination of the resulting matrix by ESR has been described earlier.[5] In the present series of experiments, Li atoms were vaporized from a resistively heated (~550 C) stainless steel tube and were trapped in argon matrices containing HCN (or CH_3CN). All the ESR spectra reported here were obtained while the matrix was maintained at ~4 K. The spectrometer frequency locked to the sample cavity was 9.425 GHz. For photoirradiation of the matrix, a high-pressure Xe−Hg lamp (Oriel, 1 kW unit) was used. The light beam was passed through a water filter, followed by a broad band interference filter of choice, and was focused on the coldfinger ~40 cm away.

A *dry HCN* was synthesized by a novel one-step process in which Fomblin Z-DIAC (perfluoropolyalkyl ether with carboxylic acid end groups) and KCN powder were mixed. $K^{13}CN$ (enrichment ≅98%, obtained form Cambridge Isotope) was used for the synthesis of $H^{13}CN$. Acetonitriles (CH_3CN and CD_3CN) obtained from Aldrich Chemical were used as received. Li metal was obtained from Alfa Products, and ^{6}Li metal (enrichment > 95%) was obtained from U.S. Services, Inc.

For examination of the viable reaction passages by the semiempirical SCF molecular orbital method, the MNDO program implemented in HyperChem was used.[6] In each case the HCN (or CH_3CN) molecule was first geometry optimized and the reacting metal atom, Li, was placed ~4 Å away; the total system was then geometry optimized following the energy surface trough (the steepest decent).

Results

SCF Semiempirical Molecular Orbital Study. Geometry optimization of the reacting system, the Li atom, and the HCN molecule placed ~4 Å apart by the MNDO SCF molecular orbital method attained the following three energy minimal structures depending upon the initial disposition of the reacting components.

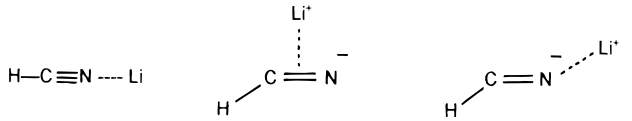

(I) (II) (III)

Complex **I** is a van der Waals type, and is formed when the Li atom approaches the nitrogen atom along the axis coincident with the CN bond. Complex **II** is formed when the Li atom is placed aside the HCN molecule closer to the carbon. As in the Li/acetylene case discussed above, the Li atom initially added to the carbon atom to form an adduct of the vinyl form; the charge transfer occurred as the vinyl form was attained; and finally the resulting Li ion moved to the position of the side-on complex. Complex **III** is formed when the Li atom is similarly placed aside the HCN molecule but closer to the nitrogen atom. The heats of complexation given by the calculations are 46, 163, and 113 kJ/mol for complexes **I**, **II**, and **III**, respectively.

The calculations further revealed that, in complex **I**, the unpaired electron is in an sp hybridized Li orbital projected away from the nitrogen, while in both complexes **II** and **III** the unpaired electron is in the in-plane antibonding π orbital of the CN moiety. The conversion of **III** to **II** is thus a symmetry allowed process, and the transition state given by the theory is only 8 kJ/mol above complex **III**. It is thus anticipated that, in the Li/HCN/Ar system wherein Li atoms and HCN molecules are co-condensed in argon matrixes at ~4 K, the most likely complexes formed are the end-on complex **I** and the side-on complex **II**.

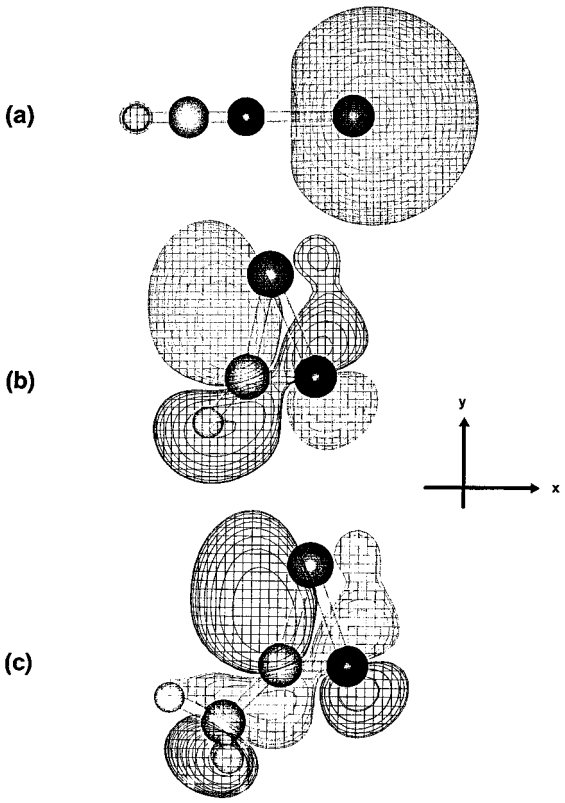

Figure 1. Isosurface contours of singly occupied molecular orbitals (SOMO) of (a) the end-on complex between HCN and Li, (b) the side-on complex between Li and HCN, and (c) the side-on complex between Li and CH_3CN.

The LCAO description of the singly occupied molecular orbital (SOMO) of complex **I** predicted by the MNDO calculation is given in eq 1. The isosurface contour of the orbital is

$$\Phi(\mathbf{I}) = a\mathrm{Li}(2s) - b\mathrm{Li}(2p_x) - c\mathrm{N}(2s) \qquad (1)$$

where $a^2 = 0.92$, $b^2 = 0.04$, and $c^2 = 0.02$

shown in Figure 1a. The ESR spectral pattern of complex **I** should thus be dominated by the hyperfine coupling (hfc) interaction with the ^{7}Li nucleus ($I = {}^3/_2$). The spin density being mostly in its 2s orbital, the hfc tensor would be essentially isotropic, its magnitude proportionately lessened from that of isolated Li atoms. The ESR spectrum of Li atoms isolated in an argon matrix had been observed earlier by Jen et al.[7] They observed two major trapping sites of Li atoms in argon matrices with the respective ^{7}Li hfc constants of 141 and 148 G. The ESR spectrum of complex **I** might also reveal a small additional isotropic hfc interaction with the ^{14}N nucleus ($I = 1$).

The LCAO description of the SOMO of complex **II** predicted by the MNDO calculation is given in eq 2. The isosurface contour of the orbital is shown in Figure 1b. The overall spectral pattern of complex **II** is then expected to be determined by the hfc tensors of the ^{14}N and proton nuclei. The hfc tensors of

(5) Kasai, P. H. *Acc. Chem. Res.* **1971**, *4*, 329.
(6) *HyperChem* (release 5); Hypercube, Inc.: Gainsville, FL, 1996.
(7) Jen, C. K.; Bowers, V. A.; Cochran, E. L.; Foner, S. N. *Phys. Rev.* **1962**, *126*, 1749.

$$\Phi(\mathbf{II}) = a\mathrm{N}(2p_y) - b\mathrm{C}(2p_y) - c\mathrm{C}(2s) + d\mathrm{H}(1s) + e\mathrm{Li}(2p_x)$$

where

$$a^2 = 0.43,\ b^2 = 0.29,\ c^2 = 0.04,\ d^2 = 0.14,\ \text{and}\ e^2 = 0.08$$

these nuclei should be very similar to those of the methylene imino radical, $H_2CN^{\bullet}$.[8]

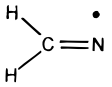

The ^{14}N hfc tensor would have an extreme uniaxial asymmetry ($\mathbf{A}_{\|} \gg \mathbf{A}_{\perp} \cong 0$), a characteristic of a situation where the unpaired electron distribution in its vicinity involves only a N(2p) orbital and no N(2s) orbital. The proton hfc tensor would be essentially isotropic and is unusually large due to a large overlap between the H(1s) orbital and the N($2p_y$) orbital. For the methylene imino radical it has been determined that $\mathbf{A}_{\|}(\mathrm{N}) = 34$ G, $\mathbf{A}_{\perp}(\mathrm{N}) \cong 0$ G, and $\mathbf{A}(\mathrm{H}) = 87$ G.[8] The actual spectral pattern of complex **II** might be broadened and/or complicated further by a small anisotropic hfc interaction with the ^7Li nucleus.

Results basically identical to those given above were obtained when similar computations were performed for the Li atom and the acetonitrile molecule. The isosurface contour of SOMO of complex **II** obtained with acetonitrile is shown in Figure 1c. The overall spectral pattern of this complex would be determined mostly by the nitrogen hfc tensor of extreme uniaxial asymmetry.

ESR Study of the Li/HCN/Ar System. (a) General Observation. When the HCN concentration (relative to argon) was less than 1 mol %, the ESR spectrum of the Li/HCN/argon system observed as prepared was dominated by the signals due to isolated Li atoms. Irradiation of such matrices with red light ($\lambda = 700 \pm 50$ nm) resulted in total disappearance of the signals due to Li atoms, and appearance of strong signals due to hydrogen atoms and methylene imino radicals, $H_2CN^{\bullet}$. The technique of co-condensing metal atoms of low ionization potential and molecules with some electron affinity in an argon matrix and effecting electron transfer between them by mild radiation, thus generating *chemically isolated* metal cations and molecular anions, had been demonstrated some time ago.[6] When the acceptor molecules are of the form HX (where X is a strong electrophile), the dissociative electron capture, $HX + e^- \rightarrow H^{\bullet} + X^-$, often occurs spontaneously. The photoinduction of H_2CN radicals observed here is thus attributed to the following sequence of events.

$$\mathrm{Li} + \mathrm{HCN} \rightarrow \mathrm{Li}^+ + \mathrm{H}^{\bullet} + \mathrm{CN}^-$$

$$\mathrm{H}^{\bullet} + \mathrm{HCN} \rightarrow \mathrm{H_2C{=}N}^{\bullet}$$

The 2s $\rightarrow$ 2p transition of the Li atom occurs at $\lambda = 670$ nm. It should be noted that the electron transfer stipulated here occurs between Li atoms and HCN molecules that are separated.

Shown in Figure 2a is the ESR spectrum of the Li/HCN-(2%)/Ar system observed as prepared. The signals due to isolated ^7Li atoms ($I = {}^3/_2$, natural abundance = 92.6%, and $\mu = 3.256\ \beta_n$) are indicated by the letter L, and those due to inadvertently formed hydrogen atoms and methylene imino radicals, H_2CN, are indicated by the letters H and M, respectively. Some electron transfer must occur when the Li beam and the HCN/Ar beam (of high HCN concentration) collide above the coldfinger. The remaining signals were observed only for matrices with a high HCN concentration and were (tentatively) assigned to the quartet due to the end-on complex **I**, and the broad doublet due to the side-on complex **II**, as indicated. Figure 2b shows the ESR spectrum of the same matrix observed after it had been irradiated with near-IR light ($\lambda = 850 \pm 50$ nm) for 20 min. The irradiation led to elimination of the quartet ascribed to complex **I**, and an increase of the doublet ascribed to complex **II**. Figure 2c shows the ESR spectrum of the same matrix observed after it had subsequently been irradiated with red light ($\lambda = 700 \pm 50$ nm) for 20 min. The second irradiation results in complete elimination of the signals due to Li atoms, an increase of the signals due to H_2CN (M), and a conspicuous increase of the doublet due to hydrogen atoms (H). We thus surmise that (1) complexes **I** and **II** are formed spontaneously from Li atoms and HCN molecules trapped close by, (2) photoexcitation of complex **I** by near-IR light ($\lambda = 850 \pm 50$ nm) leads to its conversion to

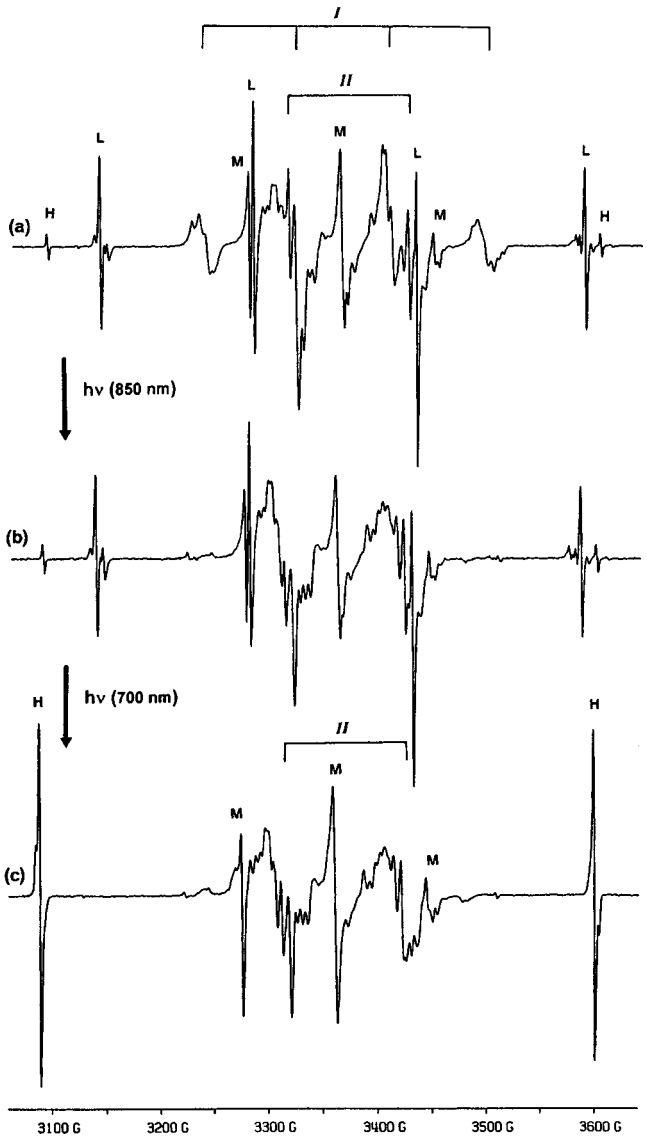

Figure 2. ESR spectra observed from the Li/HCN(2%)/Ar system: (a) immediately after deposition, (b) after irradiation with near-IR light ($\lambda = 850 \pm 50$ nm) for 20 min, and (c) after subsequent irradiation with red light ($\lambda = 700 \pm 50$ nm) for 20 min. The signals due to isolated hydrogen atoms, ^7Li atoms, and methylene imino radicals, $H_2CN^{\bullet}$, are indicated by the letters H, L, and M, respectively. The quartet ascribable to complex **I**, and the doublet ascribable to complex **II** are recognized as indicated.

(8) Cochran, E. L.; Adrian, F. J.; Bowers, V. A. *J. Chem. Phys.* **1962**, *36*, 1938.

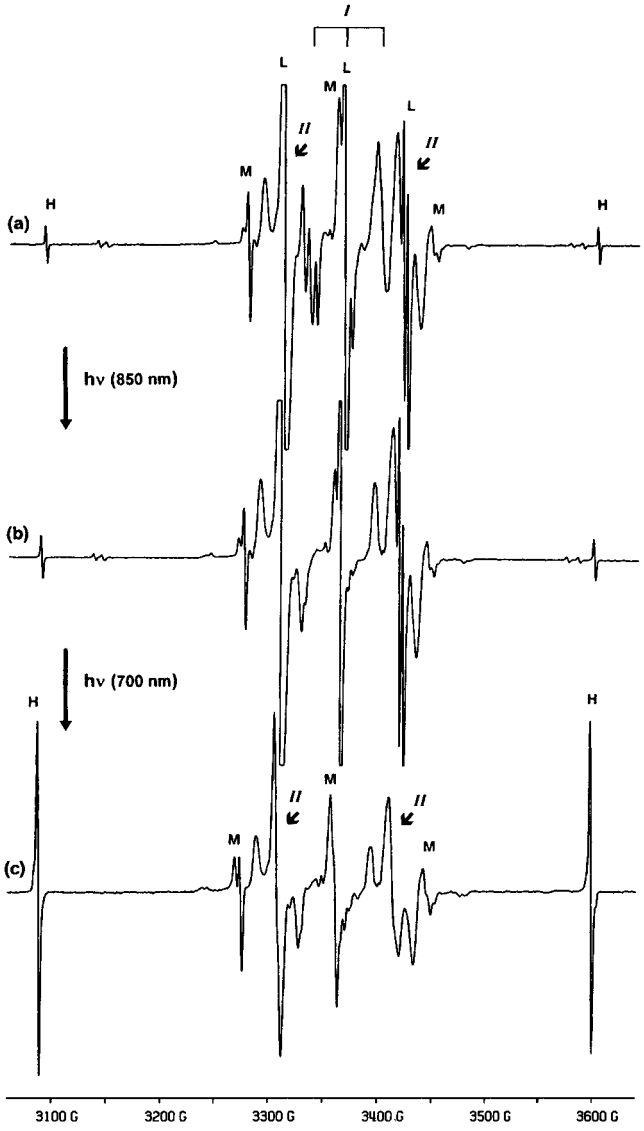

Figure 3. ESR spectra observed from the ^{6}Li/HCN(2%)/Ar system: (a) immediately after deposition, (b) after irradiation with near-IR light ($\lambda = 850 \pm 50$ nm) for 20 min, and (c) after subsequent irradiation with red light ($\lambda = 700 \pm 50$ nm) for 20 min. The signals due to isolated hydrogen atoms, ^{6}Li atoms, and methylene imino radicals, $H_2CN^{\bullet}$, are indicated by the letters H, L, and M, respectively. The triplet and the doublet ascribable to complexes **I** and **II** are also indicated.

complex **II**, and (3) photoelectron transfer is induced by red light ($\lambda = 700 \pm 50$ nm) between Li atoms and HCN molecules of further separation.

Spectra a, b, and c in Figure 3 show the corresponding spectra observed when the experiment was repeated with ^{6}Li metal (enrichment >95%). For the ^{6}Li nucleus, $I = 1$, and $\mu = 0.822$ β_n being only $\sim^1/_4$ of that of the major isotope, ^{7}Li. The signals due to isolated ^{6}Li atoms, and those due to H_2CN and hydrogen atoms, are indicated as before. The triplet pattern expected for the ^{6}Li-labeled complex **I** is readily recognized in Figure 3a. In Figure 3, spectra a and b, the signals due to complex **II** are masked by strong signals due to ^{6}Li atoms. In Figure 3c the spectral pattern of complex **II** is observed free from interference from other signals. The nitrogen hfc tensor of uniaxial asymmetry ($\mathbf{A}_{\parallel} \gg \mathbf{A}_{\perp} \cong 0$) predicted for complex **II** is now clearly revealed. Extraneous, partially resolved structures observed in the spectral pattern of ^{7}Li-complex **II** (Figure 2c) are thus attributed to the ^{7}Li hfc interaction.

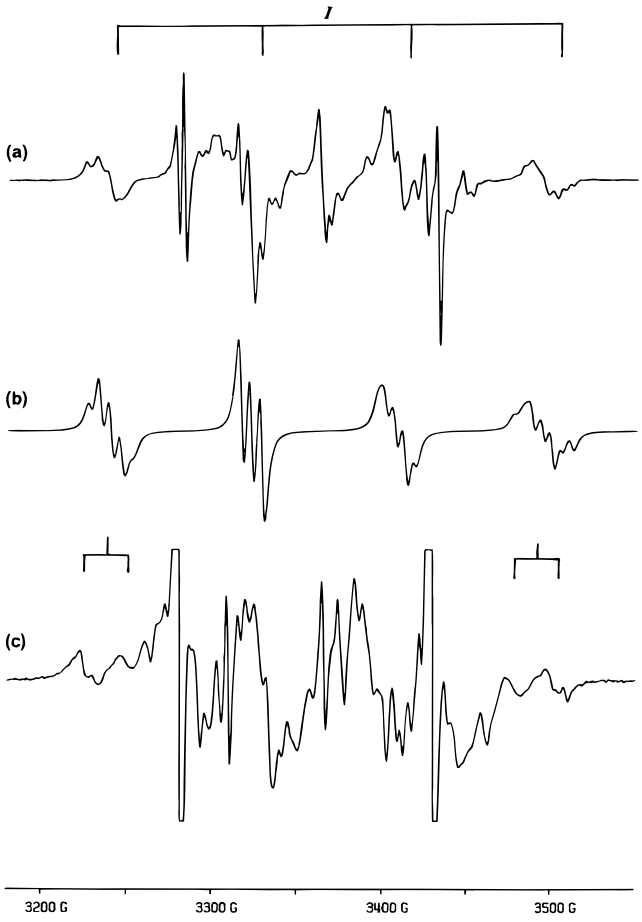

Figure 4. (a) A central section of Figure 2a encompassing the quartet due to complex **I**. (b) The simulated spectrum of complex **I** based on the parameters given in Table 1 and assuming equal occupation of the two trapping sites. (c) The spectrum (the same section) of the Li/H^{13}CN-(2%)/Ar system observed as prepared. The splitting of complex **I** signals due to the ^{13}C nucleus is recognized as indicated.

(b) Spectral Analysis of Complex I. Figure 4a shows a section of Figure 2a encompassing the quartet ascribed to complex **I**. Only the outermost components of the quartet are observed free from interference from other signals. Partially resolved features within each component are recognized as the ^{14}N hfc structures. Careful analysis of these outer components (observed in an expanded scale) led us to conclude the presence of two trapping sites with slightly different **g** and ^{7}Li hfc tensors as concluded earlier for isolated Li atoms.[7] The **g** tensors and the ^{7}Li and ^{14}N hfc tensors of complex **I** at two different sites were determined as shown in Table 1. As predicted, the Li hfc tensor is essentially isotropic and $\sim^2/_3$ of that of isolated Li atoms. A computer program that would simulate the ESR spectral pattern given by an ensemble of randomly oriented radicals ($S = {}^1/_2$) has been described earlier.[9] Figure 4b shows the computer-simulated spectrum based on these tensors (assuming equal occupation of the two trapping sites). The extra prominence of the second lowest field component results from exact coincidence of the signals of the complex at two different trapping sites. Figure 4c shows the ESR spectrum (the same section) of the Li/H^{13}CN(2%)/Ar system observed as prepared. The doublet splitting of the outermost components of complex **I** due to the ^{13}C nucleus is clearly revealed. It is concluded that the ^{13}C hfc tensor of complex **I** is essentially isotropic, and $\mathbf{A}_{iso}(^{13}C) \cong 25$ G. As for the hfc interaction due to the proton,

(9) Kasai, P. H. *J. Am. Chem. Soc.* **1972**, *94*, 5950.

Table 1. **g** Tensors and Hyperfine Coupling Tensors (given in G) of End-On Complexes HCN---Li and CH_3CN---Li Generated in Argon Matrices[a]

		tensor	∥	⊥
HCN---Li	site A	**g**	1.998(1)	1.997(1)
		A(^{7}Li)	84(2)	91(1)
		A(^{14}N)	6(1)	6(1)
	site B	**g**	1.9998(6)	1.9988(6)
		A(^{7}Li)	78(3)	85(1)
		A(^{14}N)	6(1)	6(1)
CH_3CN---Li	site A	**g**	2.0006(6)	1.9996(6)
		A(^{7}Li)	83(2)	89(1)
		A(^{14}N)	6(1)	6(1)
	site B	**g**	2.0007	1.9997(6)
		A(^{7}Li)	79(3)	85(1)
		A(^{14}N)	6(1)	6(1)

[a] For HCN---Li, it was determined that $\mathbf{A}_{iso}(^{13}C) \cong 25$ G and $A(H) \leq 2$ G. For CH_3CN---Li, it was determined that $\mathbf{A}(H) \leq 2$ G.

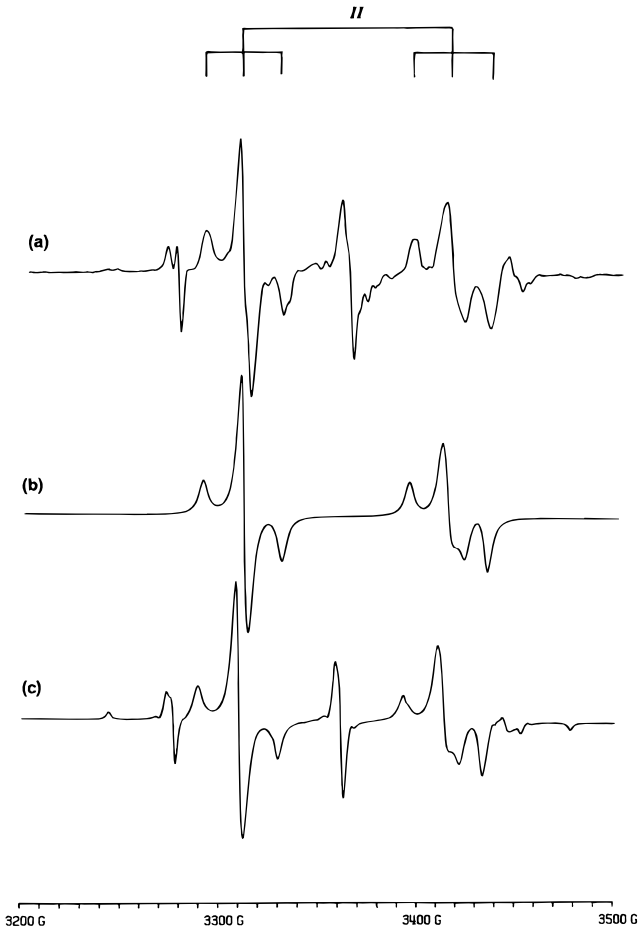

Figure 5. (a) A central section of Figure 3c encompassing the doublet-of-triplet pattern due to ^{6}Li-labeled complex **II**. (b) The simulated spectrum of complex **II** based on the parameters given in Table 2. (c) The simulated spectrum for the mixture of ^{6}Li-labeled complex **II** and H_2CN radicals with the 3/1 mol ratio.

from the line width of the lowest field component of ^{6}Li-labeled complex **I** (Figure 3a), it was concluded that $\mathbf{A}(H) \leq 3$ G.

(c) Spectral Analysis of Complex II. Figure 5a shows the central section of Figure 3c encompassing the doublet ascribed to ^{6}Li-complex **II**. The characteristic pattern due to a ^{14}N hfc tensor of uniaxial asymmetry ($\mathbf{A}_{\|} \gg \mathbf{A}_{\perp} \cong 0$) is recognized in each component of the doublet as indicated. From this doublet-of-triplet pattern, the **g** tensor and the ^{14}N and proton hfc tensors of complex **II** were determined by the simulation process iterated for the best fit. The results are given in Table 2. Figure

Table 2. **g** Tensors and Hyperfine Coupling Tensors (given in G) of Side-On Complexes Formed between the Li Atom and HCN and CH_3CN Molecules

tensor	*x*	*y*	*z*
	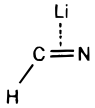		
g	1.999(1)	2.002(1)	2.004(1)
A(^{14}N)	−2.5(5)	20.0(5)	−2.5(5)
A(^{7}Li)	−3.0(5)	−4.0(5)	−7.0(5)
A(H)	109(1)	104(1)	101(1)
A(^{13}C)	32(2)	48(2)	32(2)
	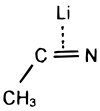		
g	2.000(1)	2.002(1)	2.002(1)
A(^{14}N)	−2.5(2)	18.5(2)	−2.5(2)
A(^{7}Li)	−2.0(3)	−4.3(3)	−7.0(3)
A(H)$_{\text{two equiv}}$	4.0(5)	6.0(5)	4.0(5)
A(H)	2.0(5)	2.0(5)	2.0(5)

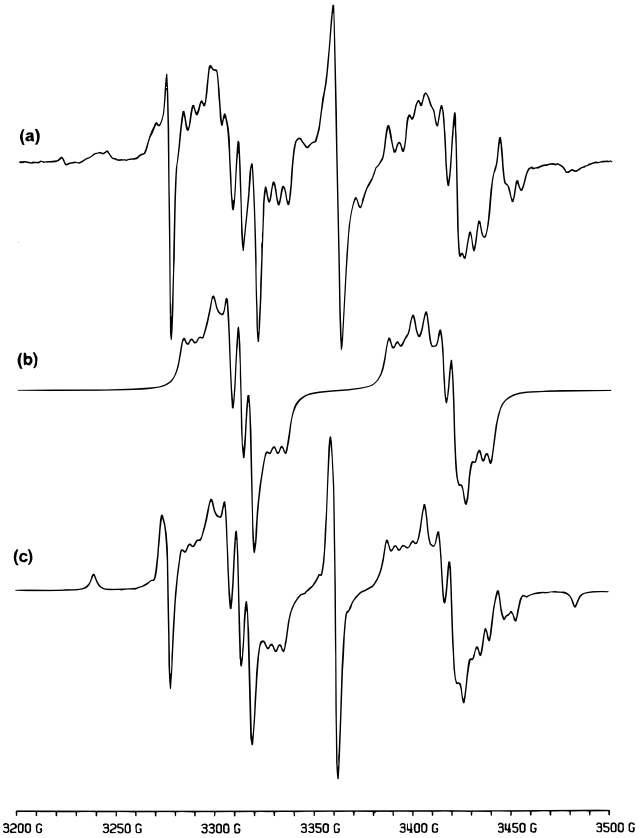

Figure 6. (a) A central section of Figure 2c encompassing the broad doublet due to ^{7}Li-complex **II**. (b) The simulated spectrum of complex **II** based on the parameters given in Table 2. (c) The simulated spectrum for the mixture of ^{7}Li-complex **II** and H_2CN radicals with the 3/1 mol ratio.

5b is the computer-simulated spectrum based on these tensors. Figure 5c is the pattern simulated for a situation where ^{6}Li-complex **II** and H_2CN radicals are present with the 3/1 mol ratio.

Figure 6a shows the central section of Figure 2c encompassing the doublet assigned to ^{7}Li-complex **II**. Using the **g** tensor and the ^{14}N and proton hfc tensors determined above, the ^{7}Li hfc tensor was determined through the iterative simulation process. The result is included in Table 2. Figure 6b shows

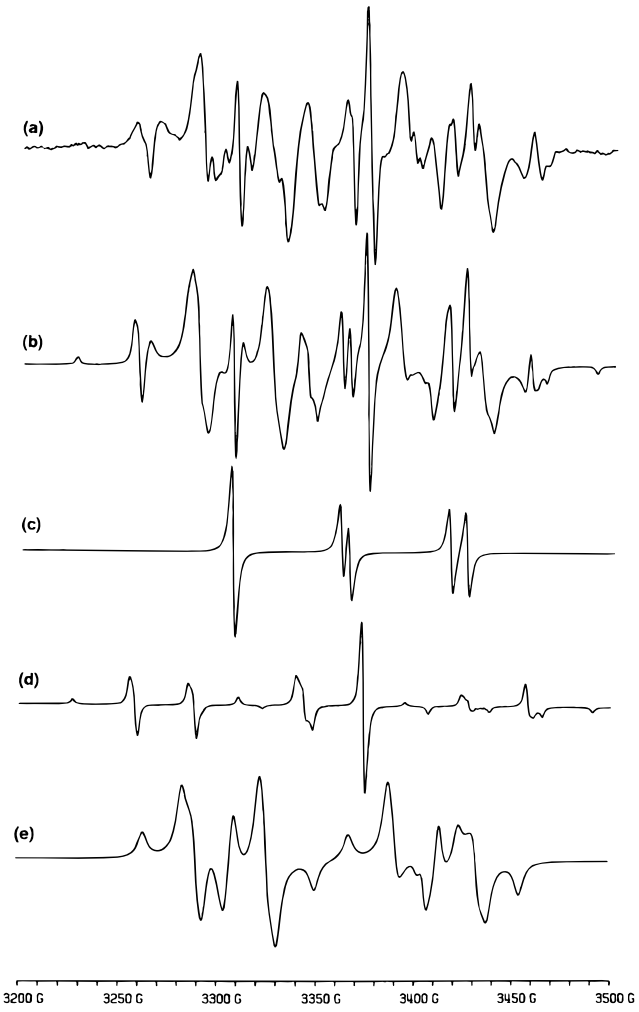

Figure 7. (a) The ESR spectrum (a central section) of the $^6Li/H^{13}CN$-(2%)/Ar system observed after irradiation with near-IR light ($\lambda = 850 \pm 50$ nm) for 20 min and with red light ($\lambda = 700 \pm 50$ nm) for 20 min. (b) The spectrum simulated for the mixture of $^6Li-^{13}C$-labeled complex **II**, ^{13}C-labeled H_2CN radicals, and residual ^6Li atoms with the molar ratio of 5:1:0.3. (c) The simulated spectrum of isolated ^6Li atoms. (d) The simulated spectrum of ^{13}C-labeled H_2CN radicals. (e) The simulated spectrum of ^6Li-^{13}C-labeled complex **II** based on the parameter given in Table 2.

the simulated spectrum of ^7Li-complex **II**. Figure 6c is the pattern simulated for a situation where ^7Li-complex **II** and H_2-CN radicals are present with the 3/1 mol ratio.

(d) Determination of the ^{13}C hfc Tensor of Complex II. Figure 7a shows the spectrum observed from the $^6Li/H^{13}CN$-(2%)/Ar system after it had been irradiated first with near-IR light ($\lambda = 850 \pm 50$ nm) for 20 min and subsequently with red light ($\lambda = 700 \pm 50$ nm) for 20 min. The total spectral pattern should be a superposition of the spectrum due to ^6Li-complex **II** split by the ^{13}C hfc tensor, the spectrum of H_2CN split by its ^{13}C hfc tensor, and perhaps the signals due to residual ^6Li atoms. Figure 7c shows the signals expected form residual ^6Li atoms. The spin Hamiltonian parameters of H_2CN, including its ^{13}C hfc tensor, were determined separately from lean spectra obtained from the Li/HCN/Ar system of low HCN concentration (<1%). The result is reported in a separate account.[10] Figure 7d shows the spectral pattern of $H_2{}^{13}CN$ simulated on the basis of the parameters so determined. Comparison of the remaining signals with those of ^6Li-complex **II** (Figure 5a) led to

(10) Kasai, P. H.; Eriksson, L. A. Submitted for publication.

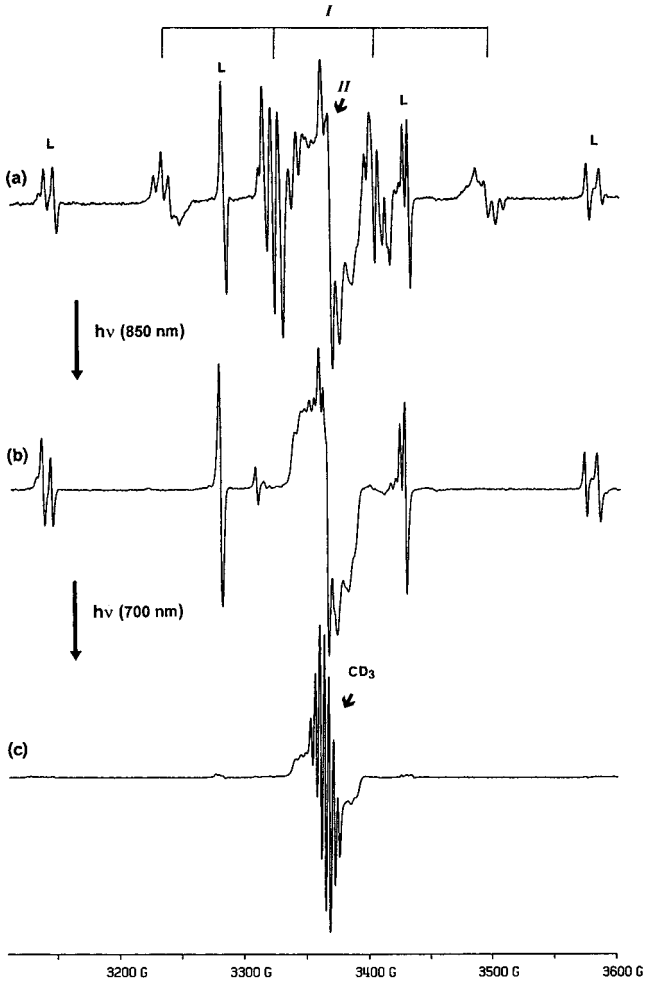

Figure 8. ESR spectra observed from the $^7Li/CD_3CN(2\%)$/Ar system: (a) immediately after deposition, (b) after irradiation with near-IR light ($\lambda = 850 \pm 50$ nm) for 20 min, and (c) after subsequent irradiation with red light ($\lambda = 700 \pm 50$ nm) for 20 min. The signals due to isolated ^7Li atoms are indicated by the letter L. The quartet ascribable to complex **I** and the broad singlet ascribable to complex **II** are recognized as indicated.

determination of the ^{13}C hfc tensor as given in Table 2. Figure 7e shows the computed pattern of $^6Li-^{13}C$-complex **II** based on the **g** tensor and the ^{14}N, ^1H, and ^{13}C hfc tensors in the table. Figure 7b shows the result of superposing the simulated spectra of $^6Li-^{13}C$-complex **II**, $H_2{}^{13}CN$, and ^6Li atoms in the respective molar ratio of 5:1:0.3.

ESR Study of the Li/Acetonitrile/Ar System. (a) **General Observation.** When the CH_3CN concentration was low (<1%), the ESR spectrum of the Li/CH_3CN/argon system observed as prepared was dominated by the signals due to isolated Li atoms. Irradiation of such matrices with red light ($\lambda = 700 \pm 50$ nm) resulted in total disappearance of the Li atom signals, and appearance of strong signals due to methyl radicals. The photoinduced change is attributed to the photoinduced electron transfer between isolated Li atoms and CH_3CN molecules, and spontaneous dissociation of the resultant anions.

$$Li + CH_3CN \rightarrow Li^+ + CH_3^{\bullet} + CN^-$$

Figure 8a shows the ESR spectrum of the Li/$CD_3CN(2\%)$/Ar system observed as prepared. The signals due to isolated ^7Li atoms, the quartet due to complex **I**, and a broad singlet ascribable to complex **II** are recognized as indicated. Here, for the quartet due to complex **I**, the nitrogen hfc structure is much

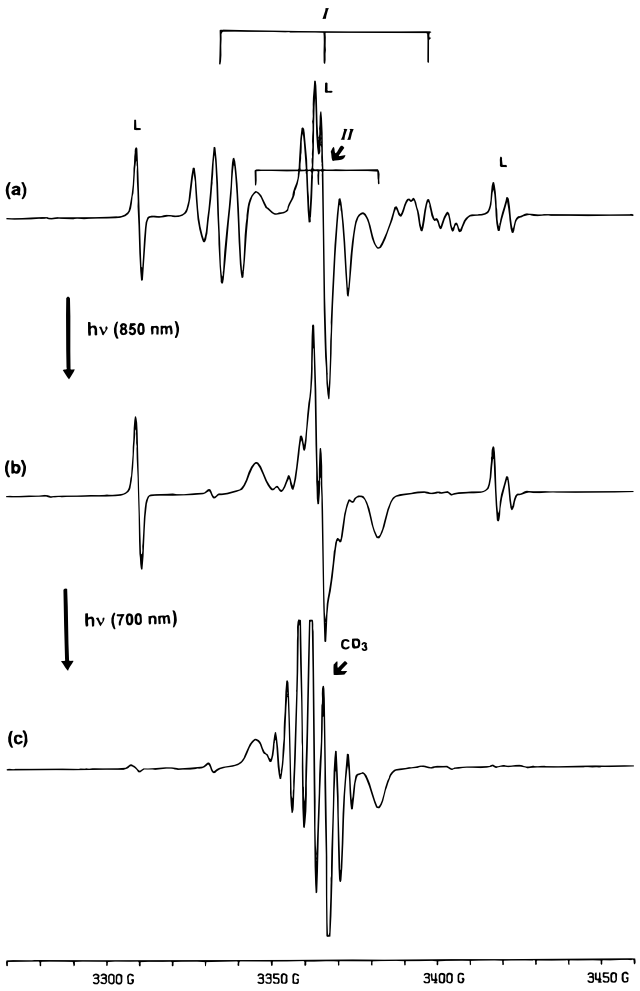

Figure 9. ESR spectra observed from the $^{6}Li/CD_3CN(2\%)/Ar$ system: (a) immediately after deposition, (b) after irradiation with near-IR light ($\lambda = 850 \pm 50$ nm) for 20 min, and (c) after subsequent irradiation with red light ($\lambda = 700 \pm 50$ nm) for 20 min. The signals due to isolated ^{6}Li atoms are indicated by the letter L. The triplet ascribable to ^{6}Li-labeled complex **I** and the triplet ascribable to ^{6}Li-labeled complex **II** are recognized as indicated.

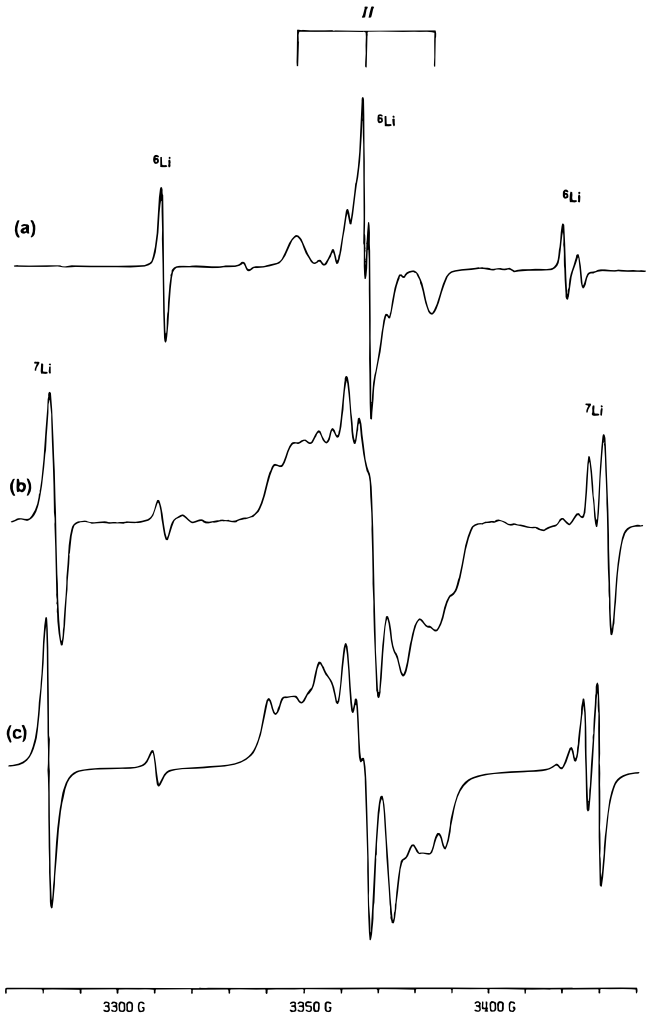

Figure 10. (a) The spectrum observed from the $^{6}Li/CD_3CN(2\%)/Ar$ system after irradiation with near-IR light ($\lambda = 850 \pm 50$ nm) for 20 min (the same as Figure 9b). (b) The spectrum observed from the $^{7}Li/CD_3CN(2\%)/Ar$ system after irradiation with near-IR light ($\lambda = 850 \pm 50$ nm) for 20 min (a central section of Figure 8b). The extra structures observed on complex II signals are ascribed to the hfc interactions with the ^{7}Li nucleus. (c) The simulated spectrum of $^{7}Li-CD_3CN$ complex **II** based on the parameters given in Table 2. The signals of isolated Li atoms are included as internal calibrations.

better resolved than that for the quartet of the corresponding complex formed in the Li/HCN/Ar system. Figure 8b shows the ESR spectrum of the same matrix observed after it had been irradiated with near-IR light ($\lambda = 850 \pm 50$ nm) for 20 min. The irradiation led to elimination of the quartet due to complex **I**, and an increase of the signals assigned to complex **II**. Figure 8c shows the ESR spectrum of the same matrix observed after it had subsequently been irradiated with red light ($\lambda = 700 \pm 50$ nm) for 20 min. The second irradiation results in complete elimination of the signals due to Li atoms, and appearance of strong signals due to methyl radicals (CD_3) at the central sector masking the major part of the spectrum due to complex **II**. The presence of complex **II** is attested by the flat shoulders flanking the CD_3 signals. We thus conclude, in exact analogy to the Li/HCN/Ar case, that (1) complexes **I** and **II** are formed spontaneously from Li atoms and acetonitrile molecules trapped near by, (2) irradiation by near-IR light ($\lambda = 850 \pm 50$ nm) leads to conversion of complex **I** to complex **II**, and (3) photoelectron transfer is induced by red light ($\lambda = 700 \pm 50$ nm) between Li atoms and acetonitrile molecules that are *chemically separated*.

Spectra a, b, and c in Figure 9 show the corresponding spectra observed when the experiment was repeated with ^{6}Li metal (enrichment >95%). The signals due to isolated ^{6}Li atoms, those due to ^{6}Li-labeled complexes **I** and **II**, and finally the signals due to CD_3 radicals are recognized as indicated.

(b) Spectral Analysis of Complex I. As in the case of the Li/HCN/Ar system, analysis of the spectral pattern due to complex **I** revealed the presence of two trapping sites with slightly different **g** and Li hfc tensors. The **g** tensors and the ^{7}Li and ^{14}N hfc tensors of complex **I** at two different sites were determined as shown in Table 1. Not unexpectedly these tensors are practically identical to those determined for complex **I** formed in the Li/HCN/Ar system. In Figure 8a the extra prominence of the second lowest field component resulting from exact coincidence of the signals of complexes at two different sites predicted earlier (Figure 4b) is revealed much more clearly. No discernible difference was observed for the spectrum of complex **I** formed in the $Li/CH_3CN/Ar$ system. From the line width of the sharpest component (the second lowest field component) of complex **I**, it was concluded that $\mathbf{A}(H) \leq 2$ G (assuming three equivalent protons).

(c) Spectral Analysis of Complex II. Figure 10a shows, in an expanded scale, the spectrum due to complex **II** observed from the $^{6}Li/CD_3CN(2\%)/Ar$ system (cf. Figure 9b). Figure

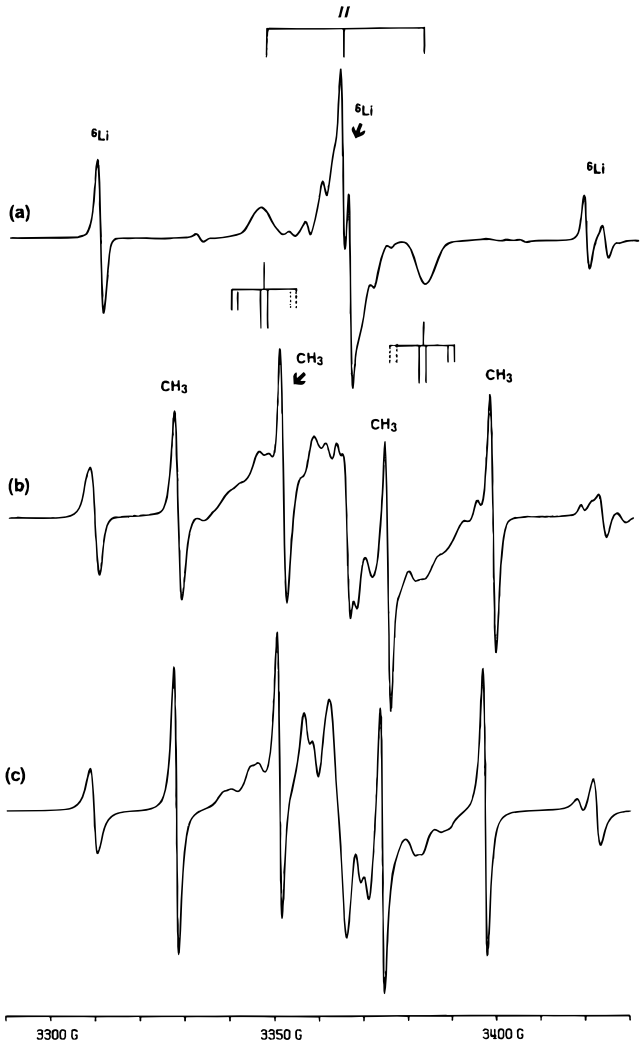

Figure 11. (a) The spectrum observed from the ^{6}Li/CD_3CN(2%)/Ar system after irradiation with near-IR light ($\lambda = 850 \pm 50$ nm) for 20 min (the same as Figure 9b). (b) The spectrum observed from the ^{6}Li/CH_3CN(2%)/Ar system after irradiation with near-IR light ($\lambda = 850 \pm 50$ nm) for 20 min and subsequent irradiation with red light ($\lambda = 700 \pm 50$ nm) for 20 min. The signals due to CH_3 radicals induced by the second irradiation are indicated. The extra structures observed on the complex **II** signals are due to the hfc interactions with the methyl protons. (c) The simulated spectrum of ^{6}Li−CH_3CN complex **II** based on the parameters given in Table 2. The signals due to isolated ^{6}Li atoms and CH_3 radicals are superimposed.

10b shows, in the same scale, the complex **II** spectrum observed from the ^{7}Li/CD_3CN(2%)/Ar system (cf. Figure 8b). From these spectra and the simulation process iterated for the best fit, the **g** tensor and the ^{14}N and ^{7}Li hfc tensors of complex **II** formed between Li and acetonitrile were determined as shown in Table 2. Figure 10c shows the spectrum of ^{7}Li-complex **II** simulated on the basis of these tensors. The signals due to ^{7}Li and ^{6}Li (naturally abundant) atoms are included as they serve the purpose of internal calibration.

Spectra a and b in Figure 11 show, in comparison, the ESR spectrum of ^{6}Li-complex **II** observed from the ^{6}Li/CD_3CN(2%)/Ar system and that observed from the ^{6}Li/CH_3CN(2%)/Ar system. The latter spectrum is that observed after irradiation with red light ($\lambda = 700 \pm 50$ nm) (hence the presence of signals due to CH_3 radicals). A close examination reveals that the characteristic pattern due to the ^{14}N hfc tensor of uniaxial asymmetry seen in Figure 11a is split further into a triplet-of-doublet in Figure 11b as indicated. The hfc interaction of ∼6 G to two equivalent protons and that of ∼2 G to the third proton are thus assessed for complex II formed between Li and CH_3-CN. Figure 11c is the spectrum simulated on the basis of these tensors. The signals due to methyl radicals and residual ^{6}Li atoms are superposed to facilitate the comparison. It is intriguing that the SOMO of this complex depicted in Figure 1c clearly indicates larger spin densities for the two equivalent protons (of the given conformation).

Discussions and Remarks

The signs of the elements of a hfc tensor cannot be determined from ESR spectra. As stated earlier, the SOMO of complex **II** given in eq 2 (and shown in Figure 1b) immediately dictates that the direction along which the largest nitrogen coupling is observed is that of the *y* axis. From the current result it cannot be determined whether $\mathbf{A}_\perp$(N) is positive or negative. From the spectrum of H_2CN generated in a single crystal of KCN and rotating about the C−N bond, Vugman et al. concluded that $A_{||}(N) = +32.2$ G and $\mathbf{A}_\perp(N) = -3.2$ G.[11] It is most likely that $\mathbf{A}_\perp$(N) determined here is also negative.

The hfc tensor of a magnetic nucleus consists of an isotropic component $\mathbf{A}_{iso}$ and an orientation dependent component $\mathbf{A}_{dip}$. A general expression representing $\mathbf{A}_{dip}$ may be written as follows.

$$\mathbf{A}_{dip} = \mathbf{g}_e\beta_e\mathbf{g}_n\beta_n\left\langle\Phi\left|\frac{1-3\cos^2\zeta}{r^3}\right|\Phi\right\rangle \cong \mathbf{g}_e\beta_e\mathbf{g}_n\beta_n\left\langle\frac{1}{r^3}\right\rangle(3\cos^2\theta - 1) \quad (3)$$

Here *r* is the distance between the unpaired electron and the magnetic nucleus, and ζ is the angle between this line and the applied magnetic field. The latter approximate form applies when the electron can be considered localized at a point away from the nucleus; θ then is the angle between the line connecting this point to the nucleus and the magnetic field. We may then conclude, based on the isosurface contour of SOMO (Figure 1b) and eq 3, that $\mathbf{A}_{dip}$ in the direction perpendicular to the molecular plane would be most negative for all the hfc tensors of complex **II**. The large, essentially isotropic hfc tensor of the proton must surely be positive as it mostly arises from the unpaired electron density in its 1s orbital. The direction along which the smallest proton hfc constant was observed was hence assigned as the *z* direction. We then note that the largest Li hf splitting is observed in this direction. The anisotropy expected from the small unpaired electron density in the Li $2p_x$ orbital is an order of magnitude smaller than the observed anisotropy. It was hence concluded that $\mathbf{A}_{iso}$(Li) was negative, and that all the elements of the Li hfc tensor were negative as shown.

The present study has clearly demonstrated that semiempirical SCF molecular orbital calculations, if used with due caution, provide a powerful method for elucidating and/or predicting the reaction process of a small system viable at the electronic ground state. For a reaction between an alkali atom (including the hydrogen atom) and a small organic molecule such as acetylene or HCN, when the reactants are far apart, the only driving force is the overlap interaction between their frontier orbitals. The frontier orbital of an alkali atom is its *n*s orbital of the unpaired electron, while the frontier orbital of the small molecule would be its highest occupied molecular orbital (HOMO). The MNDO calculation revealed that the HOMO of HCN is the bonding π

(11) Vugman, N. V.; Elia, M. F.; Muniz, R. P. A. *Mol. Phys.* **1975**, *30*, 1813.

orbital (of the CN sector) at −13.5 eV, but the orbital of the nitrogen lone pair is placed very closely at −14.3 eV. Thus when the Li atom approaches the nitrogen end of the molecule, the interaction between the Li 2s orbital and the nitrogen loan-pair orbital prevails. In either approach the driving force is the attainment of the three-electron bond, two electrons in the orbital given by the symmetric combination of the interacting orbitals and the third in the orbital given by the antisymmetric combination. The Li atom consequently acquires a net negative charge that increases with increasing approach. For complex **I** of the final structure, the MNDO calculation yielded the net atomic charge of −0.15 at the Li atom.

In the reaction process leading to the formation of complex II, the net negative charge on Li increase to −0.05 as it positions itself directly above the carbon atom. The Li → CN charge transfer and the unpaired electron density transfer then occur as the carbon moves upward to attain the vinyl structure. In the vinyl radical thus formed the Li atom has a positive charge of 0.54. The Li ion then moves toward the central, side-on position with a slight decrease in its positive charge to 0.44, reflecting the back-donation of the unpaired electron from the CN moiety into the Li $2p_x$ orbital.

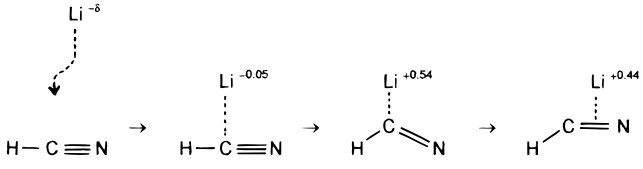

JA9807901